

TOPICS IN TOP QUARK PHYSICS ¹

J.H. Kühn

Institut für Theoretische Teilchenphysik
Universität Karlsruhe
Kaiserstr. 12, Postfach 6980
7500 Karlsruhe 1, Germany

Abstract

The status of top quark searches will be briefly reviewed. Theoretical predictions for the top quark decay rate are presented including QCD and electroweak radiative corrections. The possibilities for quarkonium searches at an hadron collider will be discussed. The perspectives for top production at an electron positron collider will be described in detail with emphasis on the behavior of the cross section and decay distribution in the threshold region.

¹Supported by BMFT Contract 056KA93P

1 Introduction

The ever-increasing energies of electron positron colliders from PETRA, PEP, and TRISTAN up to LEP as well as those of the hadron colliders $Spp\bar{p}S$ and TEVATRON have led to an impressive increase of the lower bound of the top quark mass. The limits from LEP (44.5 GeV) and from the absence of $W \rightarrow t + b$ as inferred from the W decay rate (54 GeV) are derived in a fairly model-independent way. The limits from the Tevatron on the other hand depend on the dominance of the $W \rightarrow t + b$ decay mode and hence are applicable in the context of the Minimal Standard Model (MSM) only. The mass bounds of 108 GeV from CDF and 103 GeV from D0 which have been quoted recently [1] are derived on the basis of production cross sections which in both cases are based on next-to-leading-order calculations [2]. However, the D0 limit includes recent higher-order contributions [3] which raise the cross section and increase the limit by about 5 GeV.

Precision measurements of electroweak parameters exploit the quadratic top mass dependence [4] of the ρ -parameter, resulting in [5] $m_t = 155 + 17/ - 19\text{GeV}$ with an additional error of $+17/ - 20\text{GeV}$ from the Higgs mass range between 60 GeV and 1 TeV with a central value at 200 GeV. Future top searches at the TEVATRON with increased statistics and efficiency will be able to cover this interval to a large extent and should finally be able to close the window.

Top masses above 54 GeV and below the Tevatron limit are still possible in extensions of the MSM consistent with the present data, notably in the two Higgs doublet model (THDM) where the decay mode $t \rightarrow H + b$ may dominate for m_t below 90 GeV. This window will be closed by LEP200.

The upper limit from radiative corrections may be evaded in models with negative contributions to the ρ -parameter such as THDM with large mass splittings of the type $m_S \ll m_{\pm} \ll m_{ps}$. This option will, however, be eliminated with precise experimental results for $\Gamma(Z \rightarrow b\bar{b})$.

The discovery of the top quark will not only complete the fermionic spectrum of the Standard Model. The determination of its mass will provide important input for all calculations, leaving the Higgs mass as only free parameter which could then be inferred from precise measurements planned at LEP in the near future Fig.1. Once discovered, the study of the top quark and its decay modes will constitute an important part of the physics program at the TEVATRON, LHC, SSC, and the future linear collider.

Open top quark production will be covered in the talks by Protopopescu, Harral and Froidedevaux. I will therefore concentrate on the perspectives for toponium production at the hadron collider and on the possibilities at an electron positron collider [6].

2 Top decays

Top quark physics is to a large extent dictated by the large decay rate (Fig.1), which quickly reaches its asymptotic form

$$\Gamma(t \rightarrow b + W^+) \rightarrow 175\text{MeV} \cdot \left(\frac{m_t}{m_W}\right)^3 \quad (1)$$

Three steps in the increase of the decay rate affect the qualitative behavior of top mesons [7].

i) Once m_t is above 70 GeV the hyperfine splitting between T and T^* cannot be resolved

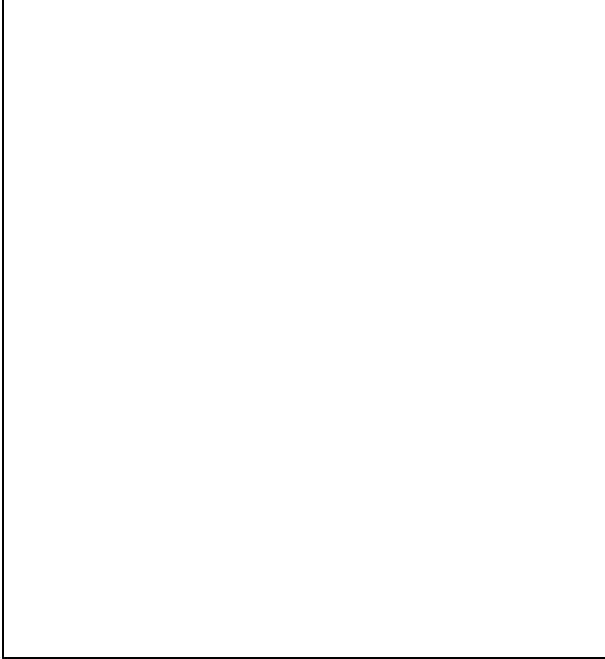


Figure 1: Solid line: The width of the top quark in the SM, including QCD and electroweak corrections and the finite W width. Dashed line: Born and narrow width approximation.

any more:

$$m_{T^*} - m_T \propto 1/m_t < 1\text{MeV} < \Gamma_t$$

The angular distribution of all decay products follow the predictions derived for a spin $1/2$ t -quark and may serve to analyze the top spin.

ii) Above 100 GeV the width exceeds 100 MeV, the characteristic scale for the formation of top mesons. No T or T^* mesons can be formed.

iii) Toponium states are severely affected once m_t is above 130 GeV, leading to a toponium width $2\Gamma_t \geq 0.88\text{GeV}$ comparable to the $1S$ - $2S$ mass difference. A complicated interplay between binding forces and the rapid decay is predicted.

m_t (GeV)	$\alpha_s(m_t)$	Γ_{nw}^{Born} (GeV)	$\delta^{(0)}$ (%)	$\delta_{QCD}^{(1)}$ (%)	δ_{ew} (%)	Γ_t (GeV)
110.0	.115	.1955	-1.44	-7.83	1.20	.1796
150.0	.110	.8852	-1.69	-8.47	1.57	.8087
190.0	.106	2.059	-1.39	-8.47	1.73	1.890

Table 1: Top width as a function of top mass and the comparison of the different approximations.

These quantitative considerations are supplemented by precise calculations including QCD and electroweak corrections to the decay rate and the spectra. A reduction of Γ_t by 7% is induced by QCD [8, 9]. Electroweak corrections increase the rate by about 1.5% [10]. The finite width of the W leads to reduction by about the same magnitude [9]. The individual corrections and the overall predictions are displayed in Table 1 for a few characteristic masses. QCD corrections including the effects from the nonvanishing Γ_W and m_b are available in the literature [8, 9]. Several sources of theoretical uncertainties remain. Not yet calculated $\mathcal{O}(\alpha_s^2)$ -terms can be estimated to contribute about 1%, the influence of the uncertainty in m_t (estimated to .5 GeV)

will induce another 1%. With an estimated experimental resolution of about 10% at best at a future linear collider, these uncertainties will not pose a serious problem in the foreseeable future.

An important issue will be the search for new decay modes expected in extensions of the Standard Model. The impact of the THDM on radiative corrections to $t \rightarrow W + b$ is fairly small [11]. For a top above 90 GeV with its large semiweak decay rate, new additional modes will manifest as admixtures to the dominant SM channel. Branching ratios of about 10% are expected for $t \rightarrow H + b$ with a plausible choice of the Yukawa coupling and similar or even smaller numbers are predicted [6] for $t \rightarrow \tilde{t} + \tilde{g}$. Exotic FCNC decays $t \rightarrow Z + c$ have been proposed [12] to exceed the SM prediction of 10^{-12} with the branching ratios ranging up to 10^{-3} or even up to 1%.

The lowest-order prediction for the energy and angular distribution of leptons from a polarized top quark in the narrow width approximation and with m_b is extremely simple and factorizes into an energy and an angular dependent term. QCD corrections to this formula are available in the literature [13] and will be of use for future experimental studies.

3 Toponium at hadron colliders

The search for η_t in its $\gamma\gamma$ decay mode has been recently proposed as a convenient tool for a precise determination of m_t at an hadron collider [14]. The small branching ratio around 10^{-4} or below, the tiny production cross section and the large background are important obstacles. The observable cross section in the $\gamma\gamma$ channel is proportional to the fourth power of the wave function at the origin and hence depends strongly on the choice of the potential. Realistic calculations based on the two loop QCD potential and including QCD corrections for production and decay have been performed recently [15]. They lead to results about a factor four below the original estimates so that this reaction will be difficult to observe in practice. The chances are more promising for quarkonium with suppressed single quark decays. The decay of a fourth generation b' boundstate into $Z + H$ for example dominates all other channels, and the resulting cross sections are large for a wide range of masses [16]. This reaction could therefore lead to the simultaneous discovery of b' and the Higgs boson.

4 Perspectives for e^+e^- collisions

Top in the continuum

The cross section for $e^+e^- \rightarrow t\bar{t}$ is fairly large throughout. It starts with a step-function-like increase to $R \approx 0.7$ at threshold as a consequence of the Coulomb enhancement $\propto 1/v$ and increases to a value of $R \approx 2$ for energies above $2m_t + 100\text{GeV}$ (Fig.2).

The production rate for $t\bar{t}$ and the number of events (for $\int \mathcal{L} dt = 10\text{fb}^{-1}$) are contrasted with the potential backgrounds $f\bar{f}$, WW and ZZ in Table 2. Detailed simulations demonstrate [17] that a ratio between signal and noise of 10 can be achieved with an efficiency of 30%. The top mass can be determined with an estimated uncertainty of about 0.5 GeV.

The large top decay rate allows for a variety of novel QCD studies. The rapid decay intercepts the evolution of the string of soft hadrons between t and \bar{t} [18]. For an extremely large top width of more than 2 GeV corresponding to m_t close to 200 GeV the string is actually spanned

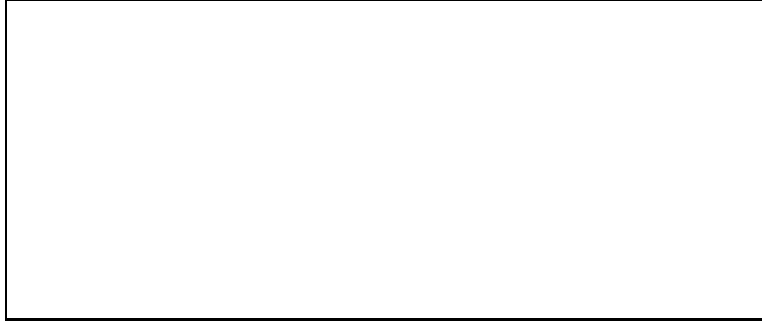


Figure 2: Cross section for $t\bar{t}$ production, including resonances, QCD corrections and initial state radiation in units of σ_{point} .

between the b and the \bar{b} such that the multiplicity depends on the invariant mass of the $b\bar{b}$ system. Perturbative soft gluon radiation is similarly affected and cut off for particular kinematic configurations [19]. This effect is particularly pronounced for e^+e^- energies in the TeV range.

Top mass (GeV)	120	150	180	150	150
$E_{c.m.}$ (GeV)	250	310	370	400	500
$t\bar{t}$	0.972	0.632	0.444	0.821	0.656
$f\bar{f}$	58.6	36.6	25.6	21.9	16.6
W^+W^-	15.2	12.5	10.3	9.46	7.44
Z^0Z^0	1.25	0.983	0.792	0.719	0.572

Table 2: Cross sections in *picobarn* for the $t\bar{t}$ signal and for the main background processes. When E_{cm} is close to the threshold (first 3 columns), the $t\bar{t}$ cross section is taken as 0.7 times the “point cross section”. Far above threshold, the cross sections are those calculated by PYTHIA. All cross sections are obtained with the inclusion of initial state radiation.

Cross section in the threshold region

A lot of effort has been invested recently in the study of the total cross section and of momentum distributions in the threshold region. For m_t above 120 GeV one faces a series of many overlapping resonances. A convenient technique to perform the summation has been proposed in [20]. The sum over the individual Breit-Wigner resonances multiplied by the wave function at the origin is easily transformed into the imaginary part of the Green’s function.

$$\sum_n |\psi_n(0)|^2 \frac{\Gamma_t}{(E_n - E)^2 + \Gamma_t^2} = \sum_n \text{Im} \frac{\psi_n(0)\psi_n^*(0)}{E_n - E - i\Gamma_t} = \text{Im}G(0, 0, E + i\Gamma) \quad (2)$$

The latter can be calculated analytically for the Coulomb and numerically for arbitrary potentials [21].

The total cross section is affected by initial state radiation that is accounted for by the standard radiator function. Electroweak corrections affect the cross section by an overall factor that can be calculated independently of the potential and other QCD effects as a consequence

of the short distance nature of W and Z exchange. Only the exchange of a light Higgs boson with large couplings may exhibit a more complicated interplay with the potential. The leading correction is in this case written as a factor

$$1 + \frac{\sqrt{2}G_F m_t^2}{4\pi} \frac{m_t}{m_H}$$

and can be traced to Coulomb-like singularity from an instantaneous Yukawa potential.

$$V(r) = \frac{\sqrt{2}G_F m_t^2}{4\pi} \frac{e^{-r m_H}}{r}$$

For realistic masses $m_t \approx 150\text{GeV}$ and $m_h > 60\text{GeV}$ retardation effects must be incorporated which are in this case as important as the $1/m_t$ term [22]. A combined treatment incorporating both the instantaneous potential and the retardation effects is given in [23].



Figure 3: Green's function $|p\mathcal{G}(p, E + i\Gamma_t)|^2$ for $m_t = 120$ and $E = -2.3$ GeV (1s peak) – solid, $E = 0$ – dotted, and $E = 2$ GeV – dashed line.

Momentum distributions

The momentum distribution of top quarks from an individual resonance can be calculated from the Fourier transform of the wave functions.

$$\left. \frac{dN}{d\vec{p}} \right|_{E=E_n} = |\tilde{\psi}_n(\vec{p})|^2 \quad (3)$$

For a series of overlapping resonances, the momentum distribution of top quarks and the decay products is again conveniently evaluated with the help of Green's functions:

$$\frac{d\sigma}{d\vec{p}}(\vec{p}, E) = \frac{3\alpha^2 Q_t^2}{\pi s m_t^2} \Gamma_t |\mathcal{G}(\vec{p}, E + i\Gamma_t)|^2 \quad (4)$$

$G(\vec{p}, E = i\Gamma)$ can be calculated numerically for complex energies and an arbitrary QCD potential by solving the Lipmann-Schwinger equation

$$\mathcal{G}(\vec{p}, E + i\Gamma_t) = \mathcal{G}_0(\vec{p}, E + i\Gamma_t) + \mathcal{G}_0(\vec{p}, E + i\Gamma_t) \int \frac{d\vec{q}}{(2\pi)^3} \tilde{V}(\vec{p} - \vec{q}) \mathcal{G}(\vec{q}, E + i\Gamma_t) \quad (5)$$

where $\tilde{V}(\vec{p})$ is the potential in momentum space. The free Hamiltonian that is used to define the Green's function \mathcal{G}_0 includes the width. The resulting momentum distribution is shown



Figure 4: *Left:* Energy dependence of $\langle p \rangle$, the average t quark momentum for $\alpha_s = 0.13$ (dotted) 0.12 (dashed) and 0.11 (solid) line for $m_t = 120$ GeV and $\Gamma_t = 0.3$ GeV.

Right: Average momentum for $\alpha_s = 0.125$ and different top masses.

in Fig.3 for a characteristic set of energies. The average momentum as a function of energy (Fig.4) depends on α_s for negative energies, that is in the binding region. Above threshold the momentum simply reflects the kinematic behavior $p = \sqrt{m_t E}$ and can be used to measure m_t independently from α_s . Up to this point final state interactions and the reduction of phase space by the $t\bar{t}$ binding have been neglected. At first sight one might expect a drastic reduction of the decay rate by about 10% from the reduction of the phase space through the potential energy of about 5 GeV. However, as argued in [25] this is largely compensated by an enhancement of the rate through final state interaction as a result of the Coulomb wave function of the outgoing b quark. A slight reduction of the rate through time dilation leads to a completely negligible change in the total cross section and the momentum distribution. Even the most pessimistic assumptions about these $\mathcal{O}(\alpha_s^2)$ corrections will, however, leave the shape of the threshold cross section unaffected, leading to a stable determination of the top mass.

In summary: An e^+e^- collider will lead to precise determination of the top mass. Top studies will provide an exciting laboratory for QCD. The determination of the $Ht\bar{t}$ Yukawa coupling will be of prime importance. The Wtb gauge coupling can be measured and limits on anomalous couplings can be derived. Novel decay modes could be searched and studied in a clean environment.

References

- [1] Quizhong Li, Linear Collider Workshop, Hawaii, April 1993.
- [2] P. Nason, S. Dawson and R. K. Ellis, *Nucl. Phys.* **B 303** (1988) 607; *ibid.* **B327** (1989) 49.
G. Altarelli, M. Diemoz, G. Martinelli and P. Nason, *Nucl. Phys.* **B 308** (1988) 724.
- [3] F.A. Berends, J.B. Tausk, W.T.Giele, *Phys. Rev.* **D 47** (1993) 2746.
- [4] M. Veltman, *Act. Phys. Pol.* **B 8** (1977) 475.
- [5] D. Schaile, Ringberg Workshop, April 1993.
- [6] for recent reviews see J.H. Kühn and P.M. Zerwas *Phys. Reports* **167** (1988) 321,
J.H. Kühn and P.M. Zerwas, In Advanced Series on Directions in High Energy Physics,
“Heavy Flavours” eds. A.J.Buras and M.Lindner, World Scientific, Singapore 1992, p.434,
J.H. Kühn et al., DESY 92-123A (1992), Vol. I, p.255.
- [7] J.H. Kühn, *Act. Phys. Pol.* **B 12** (1981) 347,
J.H. Kühn, *Act. Phys. Austr.Suppl.***XXIV** (1982) 203,
I. Bigi, Y.L. Dokshitzer, V.A. Khoze, J. Kühn, P. Zerwas, *Phys. Lett.* **B 181** (1986) 157.
- [8] M. Jezabek and J.H. Kühn, *Nucl. Phys.* **B 314** (1989) 1.
- [9] M. Jezabek and J.H. Kühn, TTP-93-4.
- [10] A. Denner and T. Sack, *Nucl. Phys.* **B 358** (1991) 46,
G. Eilam, R.R. Mendel, R. Migneron and A. Soni, *Phys. Rev. Lett.* **66** (1991) 3105.
- [11] A. Denner and A.H. Hoang *Nucl. Phys.* **B 397** (1993) 483.
- [12] H. Fritzsche, *Phys. Lett.* **B 224** (1989) 423,
W. Buchmüller and M. Gronau, *Phys. Lett.* **B 220** (1989) 641
G. Hou, these proceedings.
- [13] M. Jezabek and J.H. Kühn, *Nucl. Phys.* **B 320** (1989) 20,
A. Czarnecki, M. Jezabek and J.H. Kühn, *Nucl. Phys.* **B 351** (1991) 70.
A. Czarnecki, M. Jezabek and J.H. Kühn, *Act. Phys. Pol.* **B 20** (1989) 961.
- [14] G. Panchieri, J.-P. Revol and C. Rubbia, *Phys. Lett.* **B 277** (1992) 518.
- [15] J.H. Kühn and E. Mirkes, *Phys. Lett.* **B 286** (1992) 381, and TTP-93-4, *Nucl. Phys. B* in
print.
- [16] J.H. Kühn and E. Mirkes, TTP-93-10.
- [17] Peter Igo-Kemenes, these proceedings.
- [18] T. Sjöstrand and P.M. Zerwas, CERN-TH-6313-91.
- [19] G. Jikia, *Phys. Lett.* **B 257** (1991) 196,
V.A. Khoze, W.J. Stirling and Lynne H. Orr, *Nucl. Phys.* **B 378** (1992) 413.
- [20] V.S. Fadin, V.A. Khoze, *JETP Lett.* **46** (1987) 525, *Sov. J. Nucl. Phys.* **48** (1988) 309.
- [21] J.M. Strassler and M.E. Peskin, *Phys. Rev.* **D 43** (1991) 1500.
- [22] R.H. Guth and J.H. Kühn *Nucl. Phys.* **B 368** (1992) 38
- [23] M. Jezabek and J.H. Kühn in preparation.
- [24] M. Jezabek, J.H. Kühn and T. Teubner, *Z. Phys.* **C 56** (1992) 653,
Y. Sumino, K. Fujii, K. Hagiwara, H. Murayama, C.-K. Ng, *Phys. Rev.* **D 47** (1992) 56.
- [25] M. Jezabek and T. Teubner, Karlsruhe preprint TTP-92-38, *Z. Phys. C*, in print.